On the Utility and Disutility of JEBAR*

MARK A. CANE

Lamont-Doherty Earth Observatory, Columbia University, Palisades, New York

VLADIMIR M. KAMENKOVICH

Institute of Marine Sciences, University of Southern Mississippi, Stennis Space Center, Bay St. Louis, Mississippi

ALEXANDER KRUPITSKY

Woods Hole Oceanographic Institution, Woods Hole, Massachusetts

22 July 1996 and 18 June 1997

ABSTRACT

The usefulness of the concept of JEBAR, the joint effect of baroclinicity and relief, in large-scale ocean dynamics is critically analyzed. The authors address two questions. Does the JEBAR term properly characterize the joint impact of stratification and bottom topography on the ocean circulation? Do estimates of the JEBAR term from observational data allow reliable diagnostic calculations?

The authors give a negative answer to the first question. The JEBAR term need not give a true measure of the effect of bottom relief in a stratified ocean. A simple two-layer model provides examples. As to the second question, it is demonstrated that the large-scale pattern of the transport streamfunction is captured by the smoothed solution, especially with the Mellor et al. formulation of the JEBAR term. However, the calculated velocity field is very noisy and the relative errors are large.

1. Introduction

Since its introduction by Sarkisyan and Ivanov (1971) the concept of ''JEBAR,'' the joint effect of baroclinicity and relief, has had a venerable history as an interpretive tool in ocean circulation theoretical and diagnostic studies. An interesting recent diagnostic example is Greatbatch et al. (1991), who claim that the effect of JEBAR on changes in ocean transport in the North Atlantic over a recent 5-yr period far exceeded the influence of the wind stress. Recent examples of the use of JEBAR in the analysis of the ocean circulation include Krupitsky and Cane (1997), as well as Slørdal and Weber (1996), Myers et al. (1996), and Sakamoto and Yamagata (1996). The purpose of this note is to point out that JEBAR need not be a proper measure of the influence of topography on large-scale oceanic flows. A related issue is the difficulty in estimating JEBAR reliably from available observations (e.g., Mellor et al. 1982).

JEBAR emerges from the derivation of the vertically integrated vorticity equation. This derivation, which we only sketch here, may be found in many places (e.g., Sarkisyan and Ivanov (1971); Mellor et al. 1982; Mertz and Wright 1992). Using the smallness of the surface displacements compared to the depth of the water column (alternately, the assumption of a rigid lid) to obtain a transport streamfunction ψ and taking the curl of the vertically integrated steady momentum equations after dividing by the ocean depth $H(x, y)$ yields

$$J(\psi, f/H) = \text{curl}(\boldsymbol{\tau}/H) + \text{JEBAR} + R, \qquad (1)$$

where J is the Jacobian, ψ is the transport streamfunction, $\rho_0\boldsymbol{\tau}$ is the wind stress, ρ_0 is the mean density, and curl denote the vertical component of the usual vector curl operator; R, which includes the effects of nonlinearities and friction, will generally be ignored in what follows. JEBAR results from a manipulation of the pressure gradient term

$$\text{JEBAR} = J\left(\int_{-H}^{0} g\frac{\rho}{\rho_0} z\, dz, \frac{1}{H}\right),$$

where ρ is the density.

Mertz and Wright (1992) have reviewed various physical interpretations of the JEBAR term. If, instead of the procedure leading to (1), we first form a vorticity equation and then vertically integrate, we obtain

* Lamont-Doherty Earth Observatory Contribution Number 5734.

Corresponding author address: Dr. Mark A. Cane, Lamont-Doherty Earth Observatory, Columbia University, P.O. Box 1000, Palisades, NY 10964-8000.
E-mail: mcane@ldeo.columbia.edu

$$\beta\psi_x = -fw_B + \text{curl}\boldsymbol{\tau} + R', \tag{2}$$

where R' includes the effects of nonlinearities and friction, and w_B is the vertical component of the flow associated with the geostrophic velocity at the ocean floor:

$$w_B = \mathbf{u}_B\cdot\boldsymbol{\nabla}(-H) = \frac{1}{\rho_0 f}J(p_B, -H).$$

Here $\mathbf{u}_B$ is the horizontal geostrophic velocity at the bottom, p_B is the pressure at the bottom, and the last relation is a consequence of geostrophy.

In this form it is evident that, R' aside, any departure from the Sverdrup balance in a flat-bottomed ocean,

$$\beta\psi_x = \text{curl}\boldsymbol{\tau}, \tag{3}$$

will depend on the angle between the isobaths and the bottom velocity or bottom isobars (cf. Mertz and Wright 1992). As a rule, we expect the flow to try to behave like Taylor columns, arranging itself to go around hills and valleys, avoiding vortex tube shrinking or stretching. Thus, we expect isolines of p_B and H to be nearly parallel.

If so, the Sverdrup relation (3) holds. The Sverdrup relation appears to be structurally quite different from (1) in that the characteristics are lines of constant f (latitude lines) rather than the f/H of (1). The wind forcing term appears as curl$\boldsymbol{\tau}$ rather than curl $(\boldsymbol{\tau}/H)$. The usual interpretation of (1) is that lines of constant f/H are characteristics for the transport streamfunction integration, and the wind stress curl and JEBAR terms on the right-hand side are forcing terms. However, since both the baroclinic structure and the transport are determined by internal dynamics, they are not independent of one another. JEBAR is not an external forcing on the same footing as the wind. (Strickly speaking, JEBAR is not a forcing term at all.) It is possible for both (1) and (3) to hold if JEBAR adjusts to the value

$$\text{JEBAR} = \left\{\frac{f}{\beta}\boldsymbol{\nabla}\left(-\int_x^{x_e}\text{curl}\boldsymbol{\tau}\,dx\right)+\boldsymbol{\tau}\right\}\times\boldsymbol{\nabla}\left(\frac{1}{H}\right), \tag{4}$$

where x_e is the coordinate of the eastern coast.

Note that satisfying the Sverdrup relation (3) is equivalent to $w_B = 0$. The term fw_B is the only term in (2) influenced by either baroclinicity or bottom relief. It vanishes in a flat-bottomed ocean with or without baroclinicity: in either case this term accounts for the effect of bottom relief. In contrast, though JEBAR is the only term in (1) influenced by baroclinicity, bottom relief appears in other terms of (1): the JEBAR term accounts for the difference between the baroclinic and barotropic solutions. If baroclinic compensation results in an approximate ''level of no motion'' at depth, then w_B will be small even if the bottom topography is not flat. In such a case (4) is approximately true and JEBAR opposes—and nearly cancels—the effect of topography in the other terms of (1).

The concept of a deep level of no motion has a long useful history in both observational and theoretical oceanography. Another indication that compensation at depth characterizes much of the real ocean appears in Godfrey's (1989) global solution based on the Sverdrup relation (3). Despite ignoring topography he obtains good agreement almost everywhere with estimates of sea level displacement based on hydrographic data and a level of no motion at 2000 m. Presumably in most of the ocean the stratification has adjusted to make (4) approximately true. In the next section we present some simple examples where this is the case and then discuss how they may apply more generally.

2. Two-layer examples

Consider a two-layer ocean with topography $H(x, y)$ that does not penetrate into the upper layer. (This assumption, while not essential to our argument, simplifies its exposition considerably.) The governing steady, linear equations are

$$f\mathbf{k}\times\rho_1 h_1\mathbf{u}_1 = -h_1\boldsymbol{\nabla}p_1 + \rho_1\boldsymbol{\tau} - \rho_1\boldsymbol{\tau}_i \tag{5}$$

$$f\mathbf{k}\times\rho_2 h_2\mathbf{u}_2 = -h_2\boldsymbol{\nabla}p_2 - \rho_2\boldsymbol{\tau}_B + \rho_2\boldsymbol{\tau}_i, \tag{6}$$

$$\boldsymbol{\nabla}\cdot(h_1\mathbf{u}_1) = \boldsymbol{\nabla}\cdot(h_2\mathbf{u}_2) = 0. \tag{7}$$

All symbols have their conventional meanings, and we have included an interfacial stress $\boldsymbol{\tau}_i = k(\mathbf{u}_1 - \mathbf{u}_2)$ and a bottom stress $\boldsymbol{\tau}_B$. Here h_1 and h_2 are the thicknesses of the first and second layers, so $h_1 + h_2 \approx H$, with exact equality if the rigid-lid approximation is made. The pressures are determined hydrostatically:

$$\boldsymbol{\nabla}p_1 = g\rho_1\boldsymbol{\nabla}\eta \tag{8}$$

$$\boldsymbol{\nabla}p_2 = g\rho_2\boldsymbol{\nabla}\eta - g'\rho_2\boldsymbol{\nabla}h_1, \tag{9}$$

where $\eta = h_1 + h_2 - \text{H}$ is the surface elevation (or, a pseudoelevation for a rigid lid) and

$$g' = g(\rho_2 - p_1)/\rho_2.$$

Summing the two momentum equations (5) and (6), dividing by H, and eliminating η leads to Eq. (1) for the vertically integrated mass transport. In this two-layer case

$$\text{JEBAR} = \frac{1}{2}g'J\left(h_1^2, \frac{1}{H}\right) = \frac{g'}{2H^2}J(H, h_1^2). \tag{10}$$

Now suppose for a moment that the ocean is flat-bottomed and the interfacial stress vanishes ($\boldsymbol{\tau}_i = 0$). Then, as is well known (e.g., Charney and Flierl 1981), the motion in the lower layer will vanish as long as there is some friction there to spin down any transients. Hence, the lower-layer pressure gradient must vanish. Then from (9) and (8), $\boldsymbol{\nabla}p_1 = g'\rho_1\boldsymbol{\nabla}h_1$ so the first term on the right in (5) may be written as $-(\frac{1}{2})\boldsymbol{\nabla}(g'\rho_1 h_1^2)$. Taking the curl of this equation eliminates the pressure gradient term, and defining a streamfunction ψ_1 for the upper layer [viz. (7)] results in the Sverdrup relation (3). Once ψ_1 is determined the momentum equation (5) may be integrated to yield the layer thickness h_1.

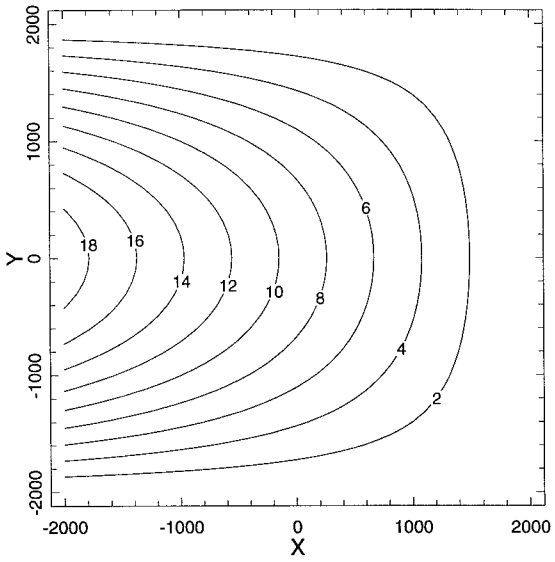

FIG. 1. The upper-layer streamfunction ψ_1 (Sv $\equiv 10^6$ m^3 s^{-1}). The exact solution (11) with parameters (13).

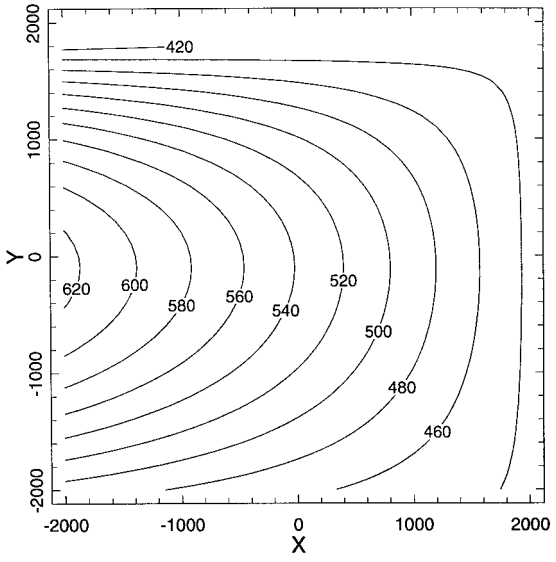

FIG. 2. The upper-layer depth h_1 (m). The exact solution (12) with parameters (13). The thickness of the upper layer in the equilibrium state was 500 m; h_e was chosen to conserve the mass of this layer.

Assuming for simplicity that the wind is zonal and depends only on the meridional coordinate

$$\psi = \psi_1 = \beta^{-1}(x_e - x)\frac{\partial \boldsymbol{\tau}^x}{\partial y}, \tag{11}$$

$$h_1^2 = h_e^2 + \frac{2f^2}{\beta g'}(x_e - x)\frac{\partial}{\partial y}\left(\frac{\boldsymbol{\tau}^x}{f}\right), \tag{12}$$

where x_e is the coordinate of the eastern boundary, and $h_e = h_1(x_e)$ is independent of y.

Now suppose that the bottom is not flat but again assume that the topography is contained in the lower layer. There is no reason why the same solution does not apply. Note that although the topography obviously does not influence the solution, JEBAR, which is given by (10), need not be zero. In fact, since we have not yet said anything about topography, H is at our disposal to make JEBAR as large as we like.

We illustrate in a square domain of length $L = 4000$ km ($-L/2 \le x \le L/2$, $-L/2 \le y \le L/2$) with bottom bathymetry $H(x)$ given by

$$H = H_0 - A\exp(-x^2/2L_H^2), \qquad L_H = 500 \text{ km},$$

$$H_0 = 4 \text{ km}, \qquad A = 0.5 \text{ km}. \tag{13}$$

The wind stress is $\boldsymbol{\tau}^x = \boldsymbol{\tau}^0 \cos(\pi y/L)$, $\boldsymbol{\tau}^0 = 10^{-4}$ m^2 s^{-2}; and the stratification is specified by $g' = 0.02$ m s^{-2}. The solutions (11), (12) are shown in Figs. 1 and 2.

While in this case, by construction, the real effect of topography is nil, the rms value of the JEBAR term is 2.2 times larger than that of the wind stress term in (1). Figure 3 shows that the JEBAR term is noticeably larger than the wind stress term outside the belt of the maximum wind stress curl.

These topographic configurations and winds are reasonably representative of realistic features. Viewing them through the JEBAR lens greatly amplifies the apparent powers of topography. One would conclude that topography is far more important than wind stress in determining the ocean transports. This is obviously not the case here: by construction, topography plays no role at all.

3. The influence of data errors

Errors are inevitable when diagnostic calculations are made from real data. These ''errors'' encompass both

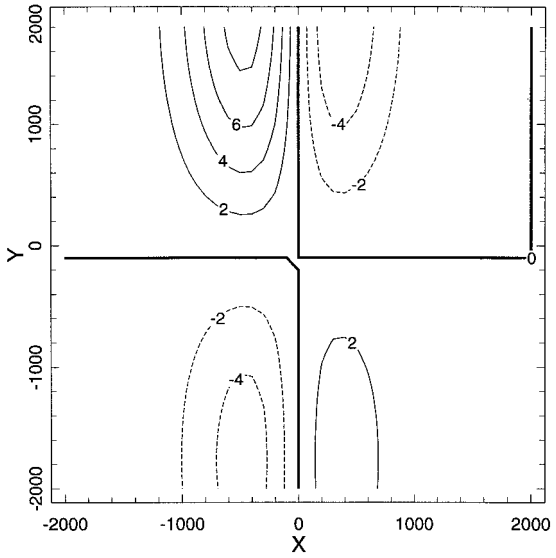

FIG. 3. The size of JEBAR normalized by the rms of curl($\boldsymbol{\tau}/H$). JEBAR is given by (10).

errors in the density measurements and uncertainties in what to choose as the appropriate value of H for each grid box of the calculation. Let the effective error in $H(x, y)$ be $\zeta(x, y)$. In the two-layer model the ''density'' variable is h_1; let its error be $\mu(x, y)$. We assume that at each grid point the expected rms errors in H and h_1 are constants, σ_H and σ_η, respectively:

$$\sigma_H = \langle \zeta^2 \rangle^{1/2}; \qquad \sigma_\eta = \langle \mu^2 \rangle^{1/2}, \tag{14}$$

where angle brackets denote the expectation operator. We further assume that the errors are uncorrelated with each other and are uncorrelated from grid point to grid point. Then, using standard centered differences to evaluate the right-hand form of Eq. (10) for JEBAR, we find the expected error in JEBAR is

$$\delta J = \langle J^2 \rangle^{1/2} = \frac{g'|h_1|}{\sqrt{2}\, dH^2} \{ [\nabla h_1]^2 \sigma_H^2 + [\nabla H]^2 \sigma_\eta^2 \}^{1/2}, \tag{15}$$

where d is the distance between grid points. In what follows we always take $d = 100$ km.

Mellor et al. (1982) suggested that one could reduce errors by rewriting (1) in terms of

$$\chi = \psi - \frac{g'}{2f} h_1^2 \tag{16}$$

(specializing their formula to the two-layer case). Then

$$\text{JEBAR} = -g' \frac{\beta}{2f} \frac{\partial}{\partial x} \left[\frac{h_1^2}{H} \right] \tag{17}$$

and the expected error in JEBAR is

$$\delta J_M = \langle J_M^2 \rangle^{1/2} = \frac{g|h_1|}{\sqrt{2}\, dH^2} \left(\frac{\beta}{f} \right) \left\{ \frac{1}{4} h_1^2 \sigma_H^2 + H^2 \sigma_h^2 \right\}^{1/2}. \tag{18}$$

The *relative errors* in JEBAR for the case of the previous section are given in Figs. 4 and 5. Different combinations of σ_H and σ_η are shown. Note that relative errors are generally higher for the traditional Eq. (15) shown in Fig. 4 than for the Mellor et al. form (18) shown in Fig. 5. In both cases the relative errors are quite high because of the sensitivity of the derivative calculations.

We expect that H has been adequately measured but that there is some error associated with its representation on a discrete grid: is the averaging used to obtain H on the grid compatible with the stratification data; is this the choice of H that is consistent with (1)? If we ignore the errors in H relative to those in the stratification data, then

$$\delta J \approx \frac{g'|h_1|}{\sqrt{2}\, dH} \left| \frac{\nabla H}{H} \right| \sigma_\eta, \tag{19}$$

$$\delta J_M \approx \frac{g'|h_1|}{\sqrt{2}\, dH} \left(\frac{\beta}{f} \right) \sigma_\eta. \tag{20}$$

Thus,

$$\frac{\delta J}{\delta J_M} = \frac{L_f}{L_T} \frac{A}{H} = \frac{L_f}{L_B}, \tag{21}$$

where L_f is the scale $f/\beta \approx a$, the earth radius; L_T is the horizontal scale of topographic features of characteristic height A; and L_B is a horizontal scale associated with the topography. For example, if H is as above [Eq. (13)] then $L_B \approx L_H(H/A)$, the scale of topographic variation multiplied by the ratio of the ocean depth to the height of topographic features.

For the scales given in (13) the Mellor et al. form reduces the error by about a factor of 1.5. Its advantage would be less for features with greater height or horizontal extent. There is an additional error introduced in the conversion from ψ to χ [Eq. (16)] of size

$$\frac{g'|h_1|}{2f} \sigma_\eta. \tag{22}$$

This error is local, whereas the errors in JEBAR accumulate: letting $\delta\chi$ denote the error in χ and δJEBAR the error in the JEBAR of Eq. (17), we have

$$J(\delta\chi,\ f/H) \approx \delta\text{JEBAR}.$$

To estimate this effect, approximate the lhs as

$$\frac{\beta}{H} \frac{\partial}{\partial x} (\delta\chi)$$

and the errors in JEBAR as in (20). After (what amounts to a random walk through) n grid points, the expected error is

$$\langle \delta\chi^2 \rangle^{1/2} \approx \frac{g'|h_1|\sigma_\eta}{2f} (2n)^{1/2}, \tag{23}$$

so the local term (22) makes only a small difference. The conclusion holds that the Mellor et al. form is advantageous as long as $L_B < L_f$.

We consider now Eq. (1) and substitute for R a small bottom friction $(\varepsilon/H_o)\nabla^2\psi$ with $\varepsilon = 10^{-6}$ s^{-1}. The influence of this term is limited to the narrow boundary layer near the western coast. In this equation we specify H and h_1 according to (13) and (12) with added white noise errors with variances $\sigma_H = 150$ m and $\sigma_\eta = 24$ m, respectively. Then we use (10) to calculate the JEBAR term and solve using the Il′in scheme (see Krupitsky et al. 1996) with a uniform grid spacing $d = 100$ km.

Both the traditional and Mellor et al. forms of JEBAR were considered. The solutions obtained were then smoothed twice in each direction with a 1–2–1 smoother (Fig. 6). The calculations showed that the errors in the terms f/H and curl $(\boldsymbol{\tau}/H)$ are negligible compared with the errors from the JEBAR term. Comparison with Fig. 1 shows that the large-scale patterns of transport streamlines are captured by the smoothed solutions, especially with the Mellor et al. formulation. However, the velocity fields are noisy and the relative errors are large. The rms relative errors in the traditional form for zonal and meridional velocity are 0.64 and 0.94, respectively. For

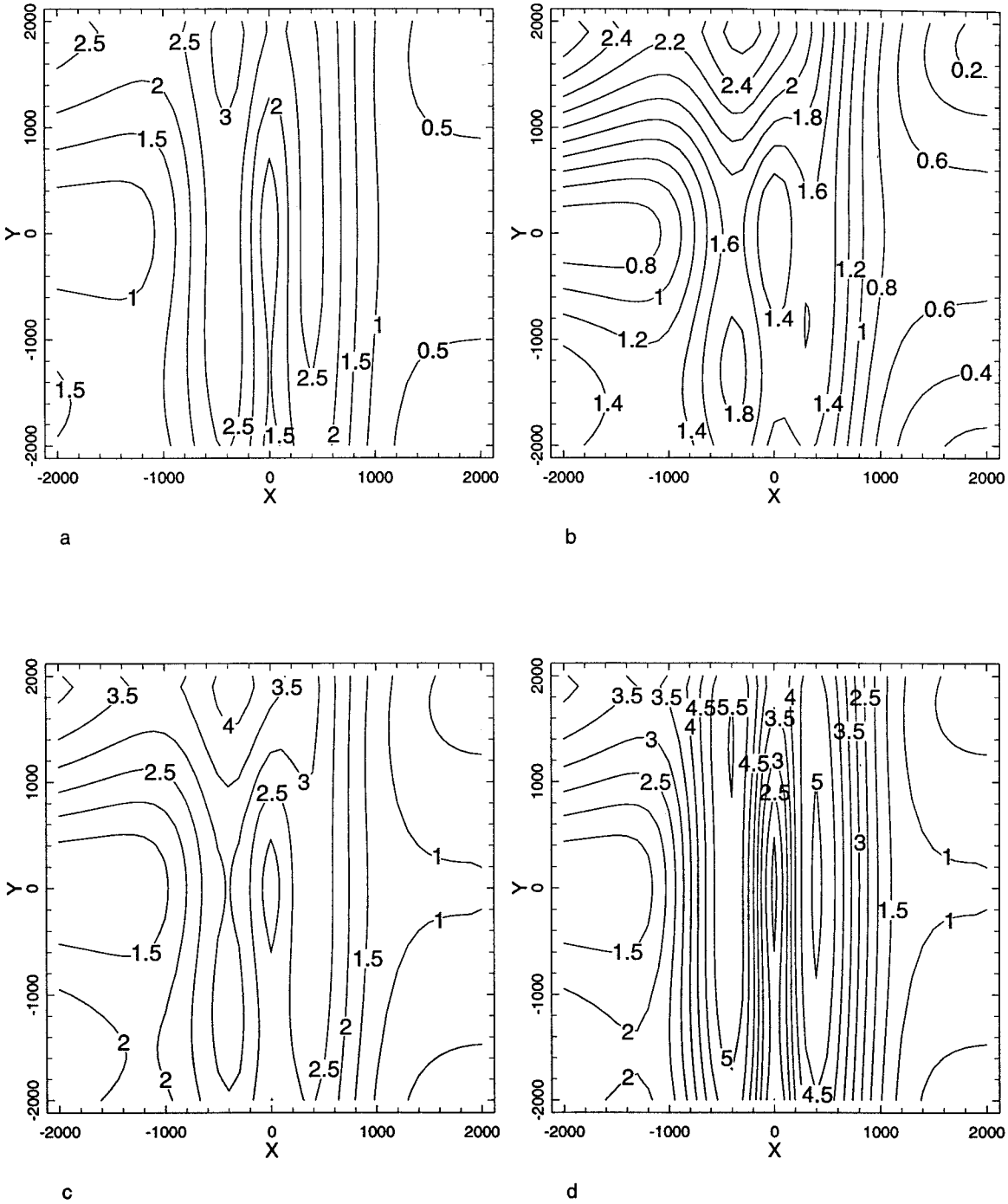

FIG. 4. The expected errors (15) in JEBAR (10), normalized by the rms of JEBAR, for various error amplitudes: (a) $\sigma_H = 100$ m, $\sigma_\eta = 10$ m; (b) $\sigma_H = 100$ m, $\sigma_\eta = 5$ m; (c) $\sigma_H = 150$ m, $\sigma_\eta = 10$ m; and (d) $\sigma_H = 150$ m, $\sigma_\eta = 20$ m.

the Mellor et al. form, the comparable numbers are 0.48 and 0.85—better, but still quite large.

4. Discussion

We have argued that JEBAR is likely to overestimate the true influence of topography on oceanic transports. We presented striking examples in the context of a two-layer model ocean. This context is idealized, but the shortcomings of the JEBAR approach that it reveals will carry over to a fully stratified ocean.

As a practical matter, we argue that this means that the transport is often better estimated by a flat-bottomed Sverdrup calculation. Such a conclusion hinges on the

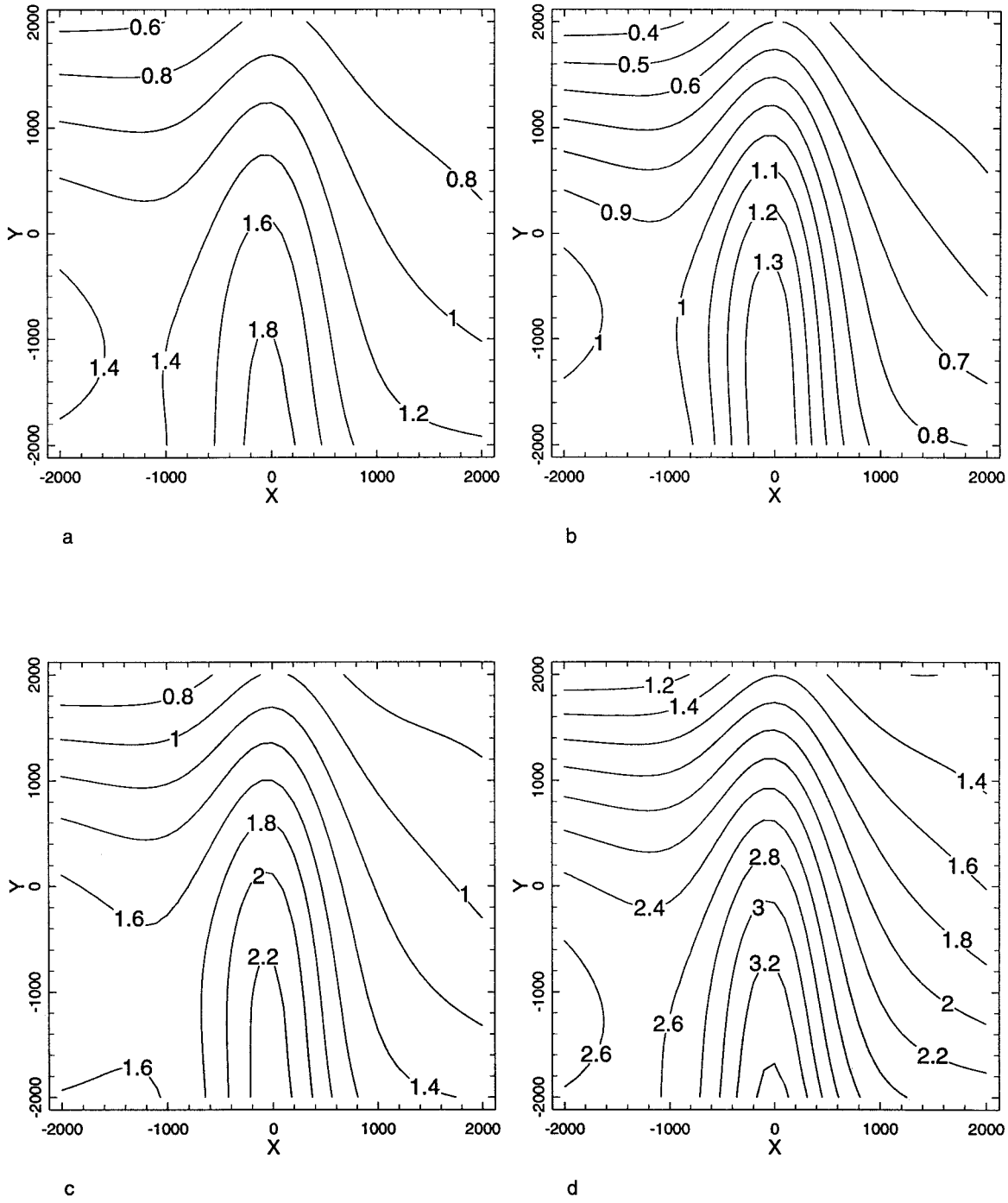

FIG. 5. As in Fig. 4 but for the Mellor et al. (1982) formulation of JEBAR (17).

transport being largely confined to the upper part of the water column, which is typically true. It is in accord with Godfrey's (1989) success in calculating surface topography while ignoring bottom topography. A somewhat different example is our study of the Antarctic Circumpolar Current (Krupitsky et al. 1996) where we obtained best agreement with the observed transports by assuming that the transport has an equivalent barotropic structure. This assumption is based on Killworth's (1992) analysis of observations and of the FRAM model output. In Krupitsky et al. the bottom influence is nonzero, but is far weaker than one would obtain from a purely barotropic calculation: the stratification shields the transport from topographic influence, but imperfectly.

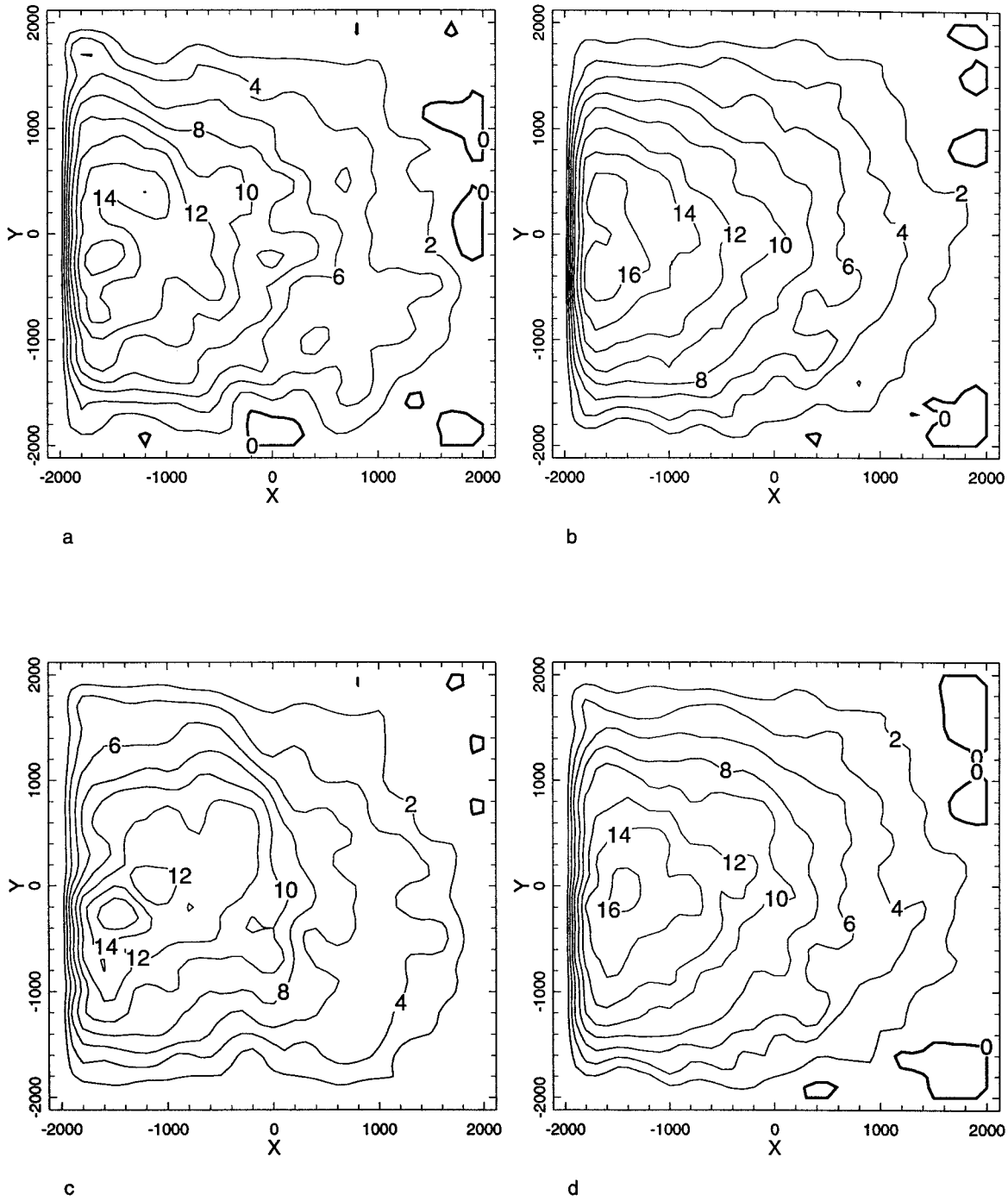

FIG. 6. The streamfunction ψ obtained by solving the streamfunction equation (1) with a small bottom drag and specified JEBAR. H and h_1 are perturbed;σ_H = 150 m, σ_η = 20 m. The solutions were smoothed by applying a 1–2–1 filter twice in each direction. (a) Regular formulation (10); f/H contours are not perturbed. (b) Mellor et al.'s formulation (17); f/H contours are not perturbed. (c) Regular formulation (10); f/H contours are perturbed. (d) Mellor et al.'s formulation (17); f/H contours are perturbed.

Our results have implications for diagnostic calculations of transport and for any numerical model that calculates a barotropic component separately from the baroclinic parts. The Eq. (1) with JEBAR is correct and can be used for the calculation. However, the results here suggest that doing so amounts to finding the influence of topography on the vertically integrated transport from the difference of two large terms: JEBAR and

$$(f\nabla\psi + \boldsymbol{\tau}) \times \nabla\left(\frac{1}{H}\right).$$

Indeed, (1) may be rewritten as

$$\beta\psi_x = \text{curl}\boldsymbol{\tau} + HR + H\left[\text{JEBAR} - (f\nabla\psi + \boldsymbol{\tau}) \times \nabla\left(\frac{1}{H}\right)\right]. \quad (24)$$

Neglecting the nonlinear and friction terms in (24) and (2), subtracting these equations and using the expression for w_B in terms of p_B yields

$$\text{JEBAR} - (f\nabla\psi + \tau) \times \nabla\left(\frac{1}{H}\right) = \frac{1}{\rho_0 H} J(p_B, H). \quad (25)$$

The baroclinic effects tend to compensate the influence of sea surface elevation gradient on the bottom pressure gradient. In the examples of section 2 the compensation is total. In the general case, ∇p_B can be very small so $J(p_B, H)$ is small as well. Given the uncertainties in data, it is unlikely that the bracketed terms on the rhs of (24) will be calculated consistently in diagnostic studies, leading to imperfect cancellation and spurious transport values. The essence of what we have to say here has been anticipated in a number of previous studies, most recently by Mertz and Wright (1992; see also references therein). In particular, one of their interpretations of JEBAR is as a correction to using the depth-averaged velocity to calculate the topographic vortex stretching instead of the correct choice, the bottom velocity $\mathbf{u}_B$. In other words, JEBAR is a measure of the deviation of the true depth-integrated motion from the hypothetical depth-integrated motion $\mathbf{u}$ of a homogeneous ocean in the same basin. Setting up this hypothetical $\mathbf{u}$ as a standard of comparison makes JEBAR a misleading measure of the true impact of the interaction of stratification and topography.

The examples of section 2 suggest that taking the flat-bottomed stratified case as a point of departure would give a better sense of the joint effect of baroclinicity and topography. Note that this is tantamount to taking a level of no motion at depth in determining a reference solution. The JEBAR approach first artificially separates the compensating effects of stratification and then regards this internal adjustment as if it were an external forcing. Diagnosing transport via JEBAR provides no constraints on the impact of inevitable data errors. Because it has a clear physical interpretation, the strategy of adding the influence of bottom velocity w_B to the Sverdrup solution suggests some plausible constraints. For example, noting the tendency of a rotating flow to go around obstacles rather than over them, one might choose to minimize w_B consistent with reasonable estimates of data errors (cf. Bogden et al. 1993, who minimized w at middepth).

Acknowledgments. This work was supported by Consortium of UCSIO (NOAA Grant NA 37GPO518) and a grant from the Vetlesen Foundation; in its later stages Alexander Krupitsky was supported by the J. Seward Johnson Postdoctoral Scholar Fellowship at the Woods Hole Oceanographic Institution. Our thanks to Virginia DiBlasi-Morris for typing this manuscript and the anonymous reviewers whose suggestions much improved our presentation.

REFERENCES

Bogden, P. S., R. E. Davis, and R. Salmon, 1993: The North Atlantic Circulation: Combining simplified dynamics with hydrographic data. *J. Mar. Res.,* **51,** 1–52.

Charney, J. G., and G. R. Flierl, 1981: Oceanic analogues of large-scale atmospheric motions. *Evolution of Physical Oceanography (Scientific Surveys in Honor of Henry Stommel),* B. A. Warren and C. Wunsch, Eds., The MIT Press, 504–548.

Godfrey, J. S., 1989: A Sverdrup model of the depth-integrated flow for the world ocean allowing for island circulations. *Geophys. Astrophys. Fluid Dyn.,* **45,** 89–112.

Greatbatch, R. J., A. F. Fanning, A. D. Goulding, and S. Levitus, 1991: A diagnosis of interpentadal circulation changes in the North Atlantic. *J. Geophys. Res.,* **96,** 22 009–22 023.

Killworth, P. D., 1992: An equivalent barotropic mode in the Fine Resolution Antarctic Model. *J. Phys. Oceanogr.,* **22,** 1379–1387.

Krupitsky, A., and M. A. Cane, 1997: A two-layer wind-driven ocean model in a multiply connected domain with bottom topography. *J. Phys. Oceanogr.,* **27,** 2395–2404.

——, V. M. Kamenkovich, N. Naik, and M. A. Cane, 1996: A linear equivalent barotropic model of the Antarctic Circumpolar Current with realistic coastlines and bottom topography. *J. Phys. Oceanogr.,* **26,** 1803–1824.

Mellor, G. L., C. R. Mechoso, and E. Keto, 1982: A diagnostic calculation of the general circulation of the Atlantic Ocean. *Deep-Sea Res.,* **29,** 1171–1192.

Mertz, G., and D. G. Wright, 1992: Interpretations of the JEBAR term. *J. Phys. Oceanogr.,* **22,** 301–305.

Myers, P. G., A. F. Fanning, and A. J. Weaver, 1996: JEBAR, bottom pressure torque, and Gulf Stream separation. *J. Phys. Oceanogr.,* **26,** 671–683.

Sakamoto, T., and T. Yamagata, 1996: Seasonal transport variations of the wind-driven circulation in a two-layer planetary geostrophic model with a continental slope. *J. Mar. Res.,* **54,** 261–284.

Sarkisyan, A. S., and V. F. Ivanov, 1971: Joint effect of baroclinicity and bottom relief as an important factor in the dynamics of sea currents (in Russian). *Izv. Acad. Sci. USSR, Atmos. Oceanic Phys.,* **7,** 116–124.

Slørdal, L. H., and J. E. Weber, 1996: Adjustment to JEBAR forcing in a rotating ocean. *J. Phys. Oceanogr.,* **26,** 657–670.